International Journal of Mass Spectrometry and Ion Processes, 92 (1989) 297–329
Elsevier Science Publishers B.V., Amsterdam – Printed in The Netherlands

^{252}Cf PLASMA DESORPTION MASS SPECTROMETRY. CONTRIBUTIONS FROM THE ROCKEFELLER UNIVERSITY *

BRIAN T. CHAIT

The Rockefeller University, 1230 York Avenue, New York, NY 10021 (U.S.A.)

(Received 31 August 1988)

ABSTRACT

The paper describes a selection of contributions made by members of Professor Frank H. Field's group in The Rockefeller University Mass Spectrometry Laboratory to both fundamental and applied aspects of ^{252}Cf plasma desorption mass spectrometry.

INTRODUCTION

In 1974 Macfarlane and Torgerson [1,2] discovered a remarkable new method for the volatization and ionization of involatile, thermally labile biomolecules. In their technique, molecular entities are desorbed and ionized directly from a solid surface by the passage of energetic ^{252}Cf fission fragments through a surface coated with a compound of interest. The technique, which has come to be known as plasma desorption mass spectrometry (PDMS) or ^{252}Cf fission fragment ionization mass spectrometry, has played a leading role in the emergence of mass spectrometry as an effective means for the characterization of underivatized biomolecules such as peptides, proteins, carbohydrates, and polynucleotides. Professor F.H. Field at The Rockefeller University was among the first members of the established mass spectrometric community to recognize the enormous potential value to biological research of the newly developed technique. He thus immediately initiated plans to construct a ^{252}Cf fission fragment ionization mass spectrometer which was put into service in 1979 [3] and has been operating effectively and fruitfully up to the present time. This paper summarizes a selection of contributions made by the group at The Rockefeller University to both fundamental and applied aspects of the mass

* Dedicated to Professor Frank H. Field on the occasion of his retirement from Rockefeller University.

0168-1176/89/$03.50

spectrometry of biomolecules using this ^{252}Cf fission fragment ionization mass spectrometer.

THE INSTRUMENT

The instrument which we constructed utilized a time-of-flight mass analyzer and was similar to that described by Macfarlane and Torgerson [4] but with some differences [5–8]. A schematic drawing of the apparatus is given in Fig. 1. The Rockefeller instrument has several noteworthy features, as follows.

The instrument incorporates a long (3 m) flight tube with an electrostatic particle guide [9] to enhance the transport efficiency of ions to the ion detector, as in the early Macfarlane and Torgerson design [4]. The long flight tube gives the mass analyzer an intrinsic resolution of ca. 2000 FWHM for ions with masses greater than 100 u, a mass determination accuracy of ca. 100 ppm, strong discrimination against energetic neutral fragments which are produced by metastable decomposition of ions during flight, and the opportunity to provide good immunity against noise from uncorrelated ions. These uncorrelated ions are generated by ^{252}Cf alpha particles, by the very high fields applied to the sample foil, and by fission fragments passing through the sample foil during a given timing cycle, subsequent to the fission fragment used to generate the time zero reference [10]. The elimination of these uncorrelated ions is achieved through the use of a set of pulsed deflection plates positioned just beyond the acceleration grids at the entrance to the flight tube (Fig. 1). A high voltage blocking potential is applied to these plates after the ions arising from a fission fragment of interest have been allowed to pass into the flight tube. Subsequently generated uncorrelated ions are then blocked for the remainder of the timing cycle.

The instrument incorporates a set of three accelerating grid electrodes positioned directly in front of the sample foil and three decelerating grid

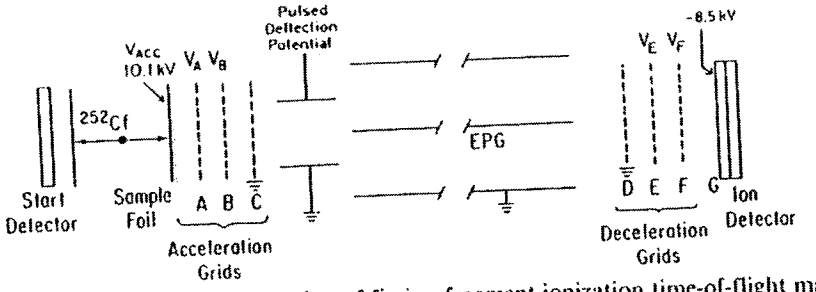

Fig. 1. Schematic representation of fission fragment ionization time-of-flight mass spectrometer. EPG is the electrostatic particle guide.

electrodes positioned just in front of the ion detector [11]. These grid electrodes allow us to study or to eliminate the ubiquitous metastable decomposition products which are an important feature of fission fragment mass spectra (see below).

Samples are inserted on a probe into the mass spectrometer through a vacuum lock with a insertion cycle time of ca. 1 min. This short cycle time is important, for example, when we wish to follow the progress of microchemical reactions taking place at the surface of solid samples (see below).

The ^{252}Cf source is purchased [12] as an electroplated layer (2 mm diameter) of californium oxide which is diffusion bonded to a 1 μm thick nickel foil and then sputter-coated with a thin layer of gold. During our initial handling of these ^{252}Cf sources, we found that it was desirable to sandwich the ^{252}Cf foil between additional 0.5 μm nickel foils to prevent self-sputtering escape of the californium [5]. Similar foil-sealed source assemblies can now be commercially acquired [12].

The time-of-flight measurements are made with a time-to-digital converter (TDC). No suitable commercially available TDC was available when we constructed our fission fragment instrument, making it necessary to design and construct a TDC in-house. The resulting device [8] has the following capabilities: time bin width, 5/8 ns; number of available time bins, $2^{21} = 2 \times 10^6$ (corresponds to a time span of up to 1.2 ms); multiple stop capability, 15 event times can be measured after a given start event; pulse pair resolution or deadtime, 7 ns; integral nonlinearity, less than seven parts in 10^7. To make full use of these capabilities we have recently interfaced the TDC to a 32-bit MicroVax I computer [13], which can store a spectrum comprised of as many as 800 000 5/8-ns channels covering a time span of 500 μs, has a dynamic range of $0-2 \times 10^9$ events per time channel, and can read and store flight times in periods of the order of tens of microseconds [14].

FISSION FRAGMENT MASS SPECTRA—DECOMPOSITION MECHANISMS

When we put our fission fragment mass spectrometer into service, little was known about the excitation of the various species desorbed and ionized by the energetic ion bombardment, or the extent to which these desorbed species decomposed and the mechanisms by which this occurred. We thus undertook a detailed investigation of the complete positive and negative mass spectra and the decomposition mechanisms of ions produced from alanine, arginine, sucrose, guanosine, 5′-adenosine monophosphate, alanylalanylalanine, and lysyltyrosylthreonine [5]. The spectra were obtained from samples introduced into the mass spectrometer in the form of thin solid films produced by electrospray deposition [15]. The mass-to-charge ratios

were measured with sufficient precision to permit deduction of atomic compositions for many of the observed fragment ions. The significant findings of the study were as follows.

(1) The amount of fragmentation occurring in fission fragment ionization even for the relatively simple molecules included in the study was large. Thus relatively low intensities of quasi-molecular ions were observed and many small fragment ions were produced with large intensities. For example, only for alanine was the intensity of the quasi-molecular ion greater than 10% of the total ionization, and for arginine the CN^- ion comprised 56% of the total negative ionization. Thus the amount of energy transferred to a large proportion of the molecules undergoing ionization must have been relatively large, and we concluded that the technique should not be looked upon only as a soft ionization method. Rather, the method appears to have a dual character with desorption and ionization involving two modes: a gentle one which produces intact quasi-molecular ions and a violent one which produces, for example, the kind of fragmentation that in the case of negative ions reduces guanosine extensively to CN^- ions.

(2) Much of the fragmentation that occurs could be rationalized in terms of established concepts of gaseous-ion chemistry. Both the positive and negative ion spectra contained mostly even-electron ions which appeared to be produced by chemical ionization-like processes and gave rise to many structurally significant fragment ion species. Thus, for example, the positive-ion spectrum of the tripeptides gave rise to the structurally informative types of ions observed earlier by Field and co-workers [16] in their study of peptide sequencing by isobutane chemical ionization.

Our first application of ^{252}Cf PDMS which used the findings outlined above involved a study of the 20-residue pore-forming peptide antibiotic alamethicin [6]. Some controversy had surrounded the elucidation of the structure of natural alamethicin, which is a mixture of closely related compounds. The study was undertaken in collaboration with Professor B.F. Gisin, who synthesized several candidate structures for the major component of alamethicin, alamethicin I. He found that one of these synthetic peptides (Fig. 2) was identical to the natural alamethicin I by a series of different criteria which included amino acid analysis, high-performance liquid chromatography, nuclear magnetic resonance spectroscopy, and biological activity. It was, however, not possible to compare the sequences directly using Edman sequence analysis because of the blocked amino-termini. We thus compared, in detail, the positive and negative ^{252}Cf fission fragment ionization mass spectra of natural and synthetic samples of alamethicin I (Fig. 3). In addition to providing molecular weight information, the positive ion spectra were found to provide detailed information on the amino acid sequences of the peptides. The close identity of these positive

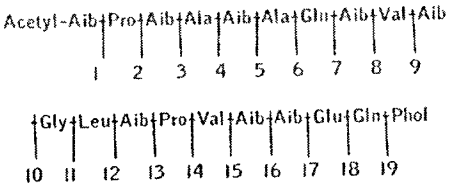

Fig. 2. Amino acid sequence of synthetic alamethicin I. Monoisotopic molecular weight = 1963.1. Aib; aminoisobutyric acid; Phol, phenylalaninol.

ion spectra from the natural and synthetic peptides then provided strong evidence that the natural and synthetic samples were indeed identical and that natural alamethicin I has the same structure as the known structure of the synthetic sample. Reaction mechanisms leading to the production of the several series of sequence ions were suggested. The chemical identities of the ions which comprise the series were again the same as or analogous to the amino terminal ions observed previously in the isobutane chemical ionization mass spectra of peptides [16] and which have come to be known as the A, B and C series in the most recent nomenclature [17]. Two of the sequence

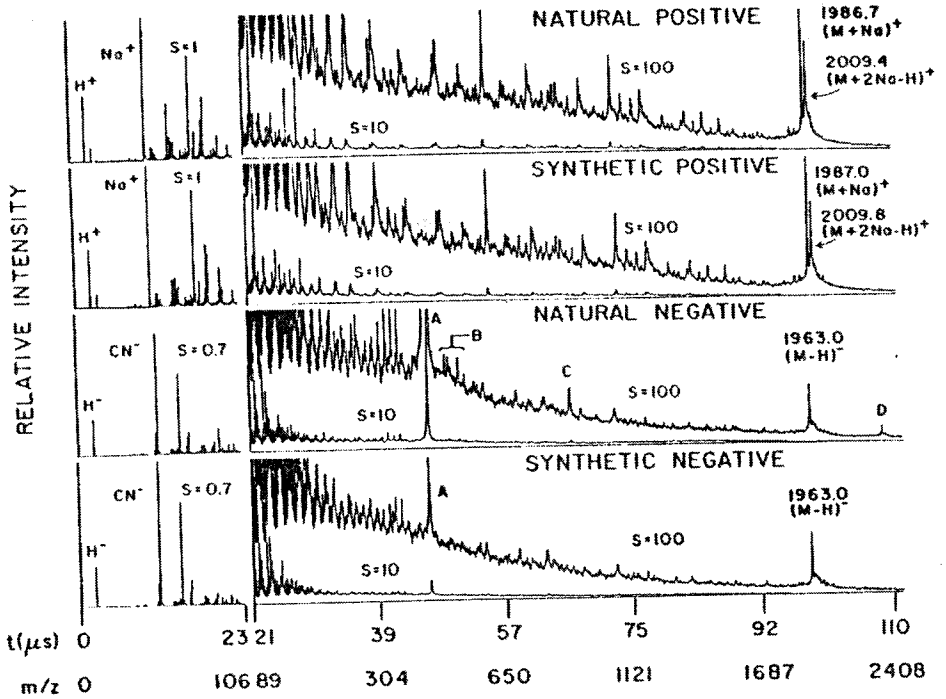

Fig. 3. Spectra of alamethicin I. S = sensitivity of intensity display. Peaks A, B and C in negative ion spectra arise from an anionic detergent impurity.

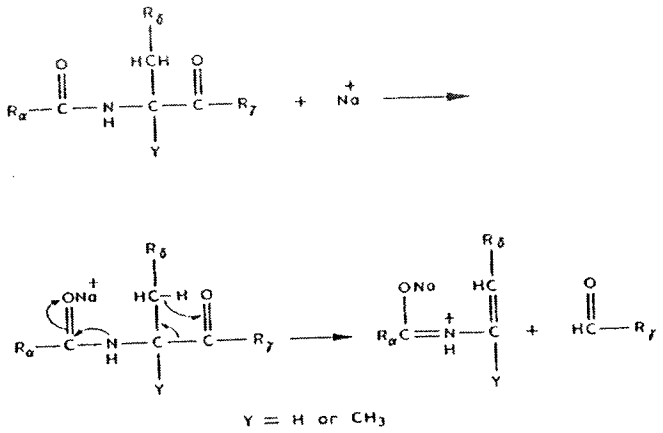

Scheme 1.

ion series (which had not previously been described) involved the addition of a sodium ion to the alamethicin I molecule followed by fragmentation with retention of the sodium in the charged fragment. The suggested reaction mechanism which leads to the most extensive series of sequence ions is given in Scheme 1. This imine fragment ion series included ions formed by breaking each of bonds 1–17 with only one exception. The ion formed by breaking bond 11 was absent from the sequence. The residue to the left of this bond is glycine, and we ascribed the absence of the ion to the fact that glycine has no hydrogen that can take part in the four-center decomposition depicted in Scheme 1.

We also observed five imine series ions produced by a variant of this reaction, as shown in Scheme 2. These variant imine fragmentations were found to occur at each residue where the component of the amino acid sidegroup R (Scheme 2) is an entity larger than H. The upper limit with this fragmentation was at bond 18.

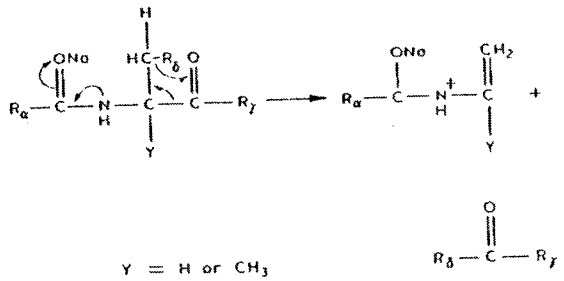

Scheme 2.

In summary, the reactions shown in Schemes 1 and 2 gave rise to sequence information complete except for ions formed by breaking bonds 11 and 19. The identity of the fragmentation spectra from natural and synthetic alamethicin I then provided strong evidence for the detailed sequence identity of the two compounds.

METASTABLE DECOMPOSITIONS

^{252}Cf mass spectra have a distinct and unusual appearance; the spectral peaks are frequently exceedingly broad and often have complex shapes. The unusual appearance of the spectra undoubtedly contributed to the slow acceptance of PDMS as a useful analytical tool. When we put our instrument into service these dominating spectral features were unexplained. We thus initiated a study of the factors affecting the peak shapes observed in our time-of-flight instrument for a series of compounds including alanylalanylalanine, guanosine, 5′-adenosine monophosphate, erythromycin, and chlorophyll *a* [7]. We hypothesized and subsequently confirmed that a major cause of the broadening is the metastable decomposition of ions in flight, with the release of internal energy as kinetic energy. Two lines of investigation were pursued to test this hypothesis. In one, the residence time of ions in the acceleration zone between the sample foil and the first acceleration grid (Fig. 1) was varied by applying appropriate potentials to the first acceleration grid. By studying the high-time tails and the peak intensities as a function of residence time we were able to detect and measure abundant unimolecular fragmentation reactions occurring within a period 5–100 ns after ion formation. In the other line of investigation, metastable fragments were separated from their parent ions on the basis of their different kinetic energies. This was accomplished by using a set of deceleration grid electrodes placed directly in front of the ion detector at the end of the flight-tube (Fig. 1). Figure 4 shows the results of this latter type of investigation obtained on the $(M + H)^+$ and $(M + Na)^+$ ions from the tripeptide AlaAlaAla (MW = 231). The spectrum shown in Fig. 4A was obtained with no potential applied to the deceleration grids and gives the normal time-of-flight spectrum of the compound. Under these experimental conditions, fragment ions and neutral species arising by metastable decomposition in the field-free flight tube have the same mean velocities as the precursor ions from which they arise. Thus the neutral and charged fragments contribute to the same peak in the velocity measuring time-of-flight instrument as do their unfragmented precursor ion species.

It is seen from Fig. 4A that the peak corresponding to the protonated molecule is substantially broader than that of the sodium-cationized species, which has a width consistent with the limiting instrumental resolution of ca.

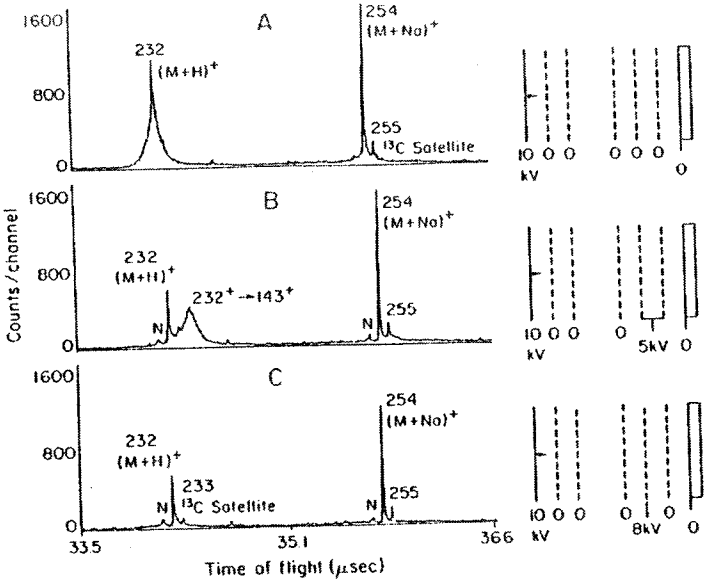

Fig. 4. Quasi-molecular ion peaks in alanylalanylalanine; $(M+H)^+$ and $(M+Na)^+$ peaks at three decelerating potentials: A, 0 V; B, 5 kV; and C, 8 kV.

2000 FWHM. The reason for the large width of the $(M+H)^+$ peak is apparent from Fig. 4B, where the applied deceleration potential has caused the original broad peak to split into three components. The small peak, labeled N, corresponds to the unretarded neutral entities. The large sharp peak corresponds primarily to unfragmented $(M+H)^+$ ions, and the broad peak corresponds to $(M+H)^+$ ions which have undergone metastable fragmentation in the field-free flight tube. As the deceleration potential is further increased, the metastable decay product ions have increasingly longer flight times with respect to the unfragmented parent ions, and they are finally suppressed altogether as shown in Fig. 4C.

In addition to providing an explanation for the origin of the broad and complex peaks observed in PDMS, several useful pieces of information on the excitation and fragmentation of ion species desorbed by fission fragments could be deduced from these and similar retardation experiments:

(1) Sodium cationization was in general shown to inject less energy into the desorbed molecule than protonation, or at least produced ions which underwent less metastable fragmentation. Thus, 82% of the $(M+H)^+$ ions of AlaAlaAla were observed to undergo flight-tube fragmentation reactions versus only 46% for the $(M+Na)^+$ species.

(2) The retardation behavior of the metastable components with respect to the precursor ion was used to deduce information on the identities of the

fragmentation pathways. Thus, for example, protonated AlaAlaAla could be shown to decay in the flight tube primarily through the single transition

$$\underset{m/z\ 232}{(M+H)^+} \rightarrow \underset{m/z\ 143}{NH_2CH(CH_3)CONHCH(CH_3)C{\equiv}O^+} + NH_2CH(CH_3)COOH$$

(3) The time spreads of the separated metastable components were used to deduce lower limits for the average amount of internal energy that was converted into translational energy for given metastable transitions. Thus, for example, a lower limit of 32 ± 9 meV was measured for the energy release which occurred during the metastable transition $232^+ \rightarrow 143^+$ shown above.

(4) From a practical point of view we demonstrated (see, e.g. Fig. 6) that the suppression of decomposition products can be used to enhance the resolution by eliminating the broad components of the peaks or separating them from the sharp components.

In an effort to widen our understanding of the behaviour of large ionized molecules produced by fission fragment bombardment, we undertook a detailed investigation of the fragmentation of chlorophyll *a* (Chl *a*), MW = 892 [11,18,19]. The normal fission fragment time-of-flight mass spectrum of Chl *a* (Fig. 5A) showed that a very high proportion of the ionized molecules undergo prompt fragmentation reactions (reactions occurring in times $< 10^{-8}$ s after the ionizing events that give rise to the sharp fragment ion peaks). The normal mass spectrum shown in Fig. 5A gives a "snapshot" of the distribution of ions formed from Chl *a* ca. 100 ns after the ion-forming event (the time required to accelerate the ions into the field-free flight tube). This "snapshot" is somewhat blurred by the subsequent metastable decomposition of many of these ions. Figure 5B shows the equivalent spectrum after all metastable fragmentation products (those fragments produced in times between 10^{-7} and 10^{-4} s after the ionizing event) have been removed. Only 22% of all ions in the mass range 400–1000 and only 1.1% of the $M^{+\cdot}$ and $(M + H)^+$ species survive the flight to the detector. The low survival rate can be seen in Fig. 6, which shows the molecule ion region of a chlorophyll *a* sample containing a small amount of pheophytin *a* (Pheo *a* = Chl *a* − Mg + 2H). In this measurement the broad metastable peaks (shown cross-hatched) have been separated from the sharp peaks which arise from ions not fragmenting in the flight tube. By measuring the time separation *t* between the broad metastable peak and its sharp precursor peak we could determine the mass of the metastable daughter ion [11,18]. In the case shown, the neutral loss from both Chl *a* and Pheo *a* was determined to be 279 ± 2 u, corresponding to the elimination of the phytyl hydrocarbon tail.

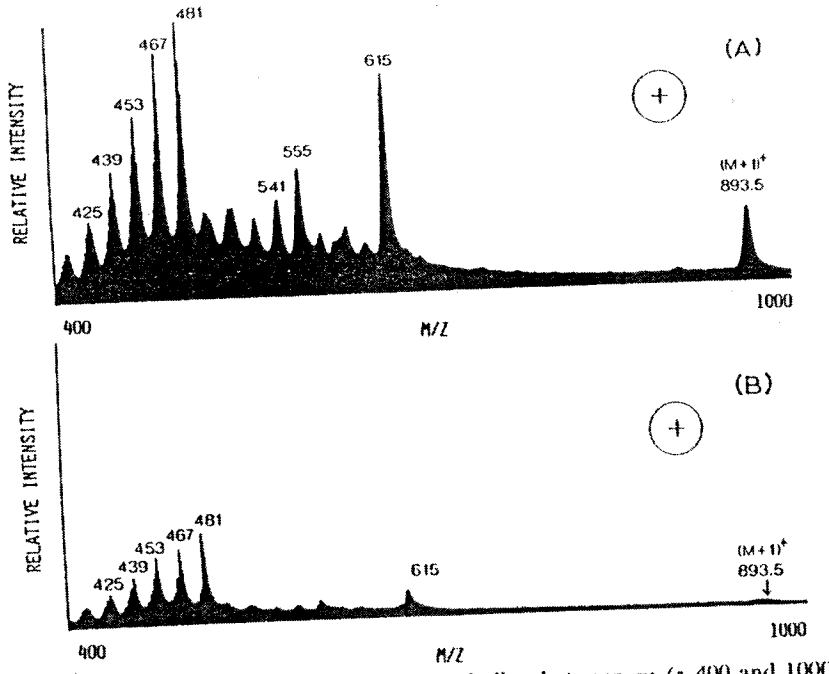

Fig. 5. Positive ion mass spectra of chlorophyll *a* between *m/z* 400 and 1000. A, spectrum taken with deceleration potential = 0. B, Spectrum taken with deceleration potential = 99% of acceleration potential.

In this way we obtained maps of most of the intense metastable fragmentation in Chl *a* for both positive (Fig. 7) and negative ions, and were able to show that much of the fragmentation could be readily rationalized by using well-known concepts of gaseous ion chemistry. Rate constants for certain

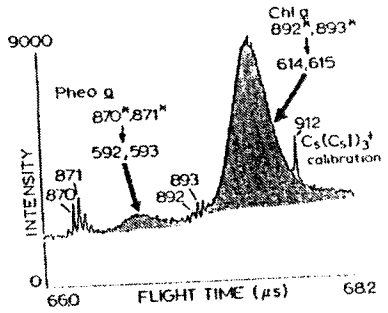

Fig. 6. Quasi-molecular ion peaks from chlorophyll *a* sample containing a small admixture of pheophytin *a*. Separation of broad peaks arising from flight-tube fragmentation products (cross-hatched) and sharp peaks arising from ions not undergoing fragmentation. The metastable transitions are indicated.

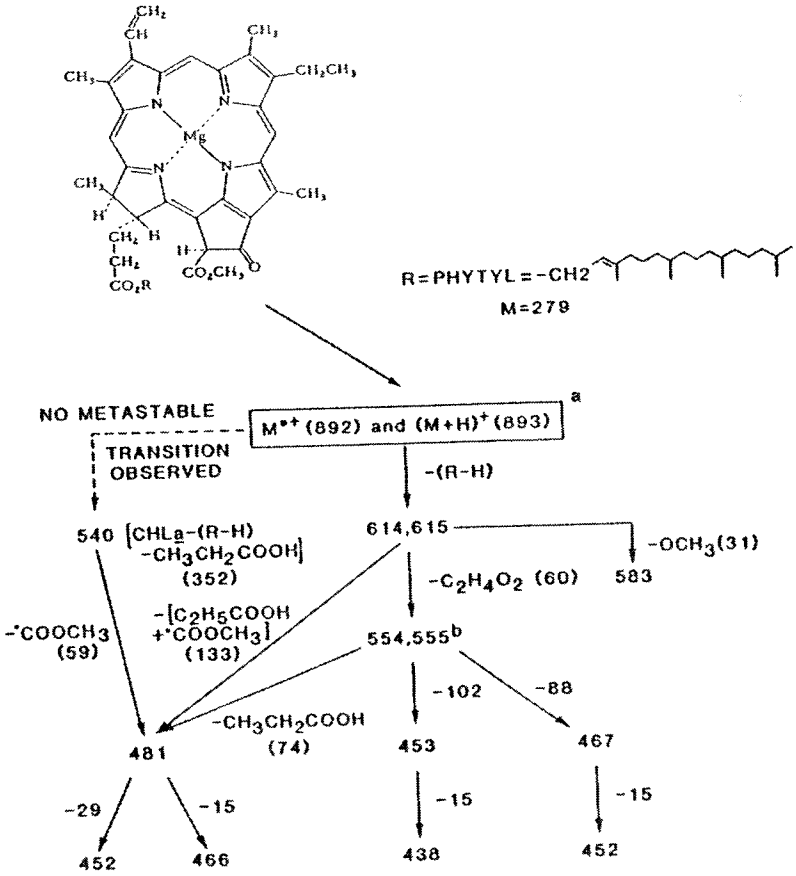

Fig. 7. Map of positive ion flight-tube fragmentation of ionized chlorophyll *a*.

fragmentation reactions were deduced from tails of peaks and from measurements which used segmented fields in the ion acceleration region. We found that fragmentation occurs with rate constants ranging from $> 10^9$ s^{-1} to 10^4 s^{-1}, and we suggested that the fission fragment induced fragmentation processes observed in Chl *a* involved many of the concepts embodied in the quasi-equilibrium theory of mass spectra, e.g. formation of reactant ions with a wide range of energies, which results in a network of sequential

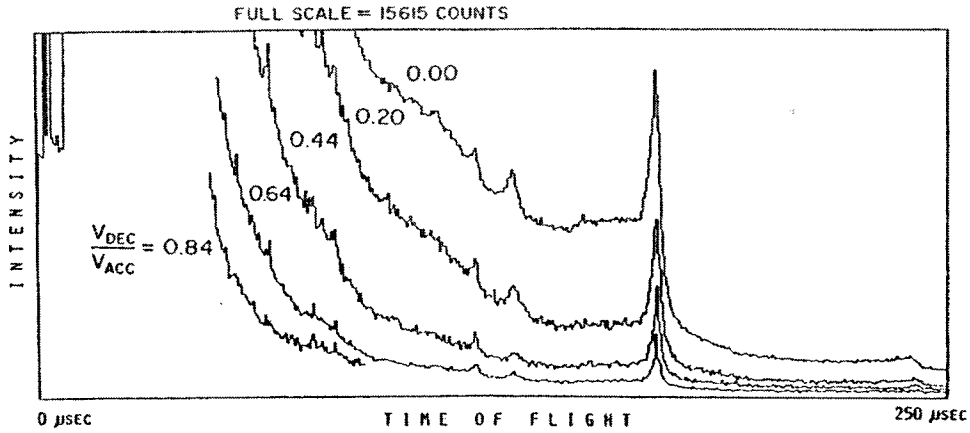

Fig. 8. Time-of-flight spectra of bovine insulin with five different magnitudes of the ratio of the deceleration potential to the acceleration potential, V_{dec}/V_{acc}. The run at 0.84 is only represented up to 90 μs for the sake of clarity.

and competing unimolecular reactions with variable and wide-ranging rate constants.

The studies described above were made on compounds with molecular weights less than 1000 u. Larger molecules are, in general, more difficult to volatilize than are smaller molecules and may therefore be expected to absorb more energy during desorption. On the other hand, larger molecules contain many more degrees of freedom and can therefore absorb more energy without undergoing fragmentation than can smaller species. To investigate the competition between these opposing effects, we extended the investigation of the metastable decomposition of fission fragment bombardment produced ions to a considerably higher molecular weight compound, i.e. the polypeptide hormone bovine insulin, which has a monoisotopic molecular weight of 5729.6 [20]. Metastable fragmentation measurements were made of the decay of the $(M + H)^+$ ion, the $(M + 2H)^{2+}$ ion, the $(2M + H)^+$ ion, intact A- and B-chain fragment ions, and ions constituting the intense continuum observed in the positive fission fragment induced mass spectrum. Figure 8 shows the effect on the time-of-flight mass spectrum of applying a series of potentials to the metastable rejection grids at the end of the flight tube (Fig. 1). Ion fragments with

$$M(\text{fragment}) < (q_D V_{dec}/q_A V_{acc}) \times M(\text{precursor}) \quad (1)$$

where q_A is the charge on the accelerated ion, q_D is the charge on the decelerated ion, V_{dec} is the deceleration potential, and V_{acc} is the acceleration potential, are reflected and are thus not detected. Clearly, both the peaks and the continuum become smaller as larger deceleration potentials are

applied, corresponding to the rejection of increasing amounts of flight-tube fragmentation products. The data indicated that only a very small percentage (< 4%), of the insulin dimer ions which survive acceleration (t_{acc} = 539 ns) subsequently survive the 240 μs flight to the detector. Similarly, < 10% of the protonated molecule ions which are still intact after 381 ns survive the remaining 170 μs flight to the detector. Almost half of the $(M + H)^+$ ions decay in flight to fragment ions with m/z < 1200. We hypothesized that many of these low-mass fragment ions are formed by sequential decay processes, as a single decay is not likely to reduce significantly the energy content per degree of freedom of a heavy fragment compared with its high-mass precursor [19]. Indeed, the A- and B-chain prompt fragment ions were found to have a similar propensity to undergo metastable decompositions as do the $(M + H)^+$ ions.

An investigation of the temporal distribution of the flight-tube fragmentations also indicated that the decays are heavily weighted to favor early times, i.e. high rate constants.

In 1985 Sundqvist, Roepstorff and co-workers [21] devised a new method for polypeptide sample preparation which yielded fission fragment mass spectra of much higher quality than that previously obtained with samples produced by electrospray deposition. The method involves the non-covalent attachment of monolayer amounts of polypeptide to a supporting matrix of nitrocellulose (NC) which has an affinity for the polypeptide. The results of these workers indicated that protonated polypeptides desorbed from NC undergo substantially less fragmentation than do polypeptides desorbed from bulk material. A strong enhancement of multiply charged (protonated) intact molecule species was also observed from NC. Two further practical benefits resulted from the use of NC. First, the sensitivity for detecting polypeptides was increased by several orders of magnitude. Second, the sensitivity of the spectral response to impurities (e.g. salts) was markedly reduced because the impurities could frequently be removed from the surface-sorbed polypeptide layer by simply rinsing the surface with clean solvent. In the hope of casting some light on the physico-chemical reasons for the improvements observed with NC, we undertook a series of comparisons between the amount of fragmentation in ions desorbed from bulk (electrosprayed) polypeptide samples and the amount of fragmentation observed in the corresponding ions desorbed from polypeptides bound to NC [22]. Figure 9 gives a comparison between the mass spectra obtained from an electrosprayed sample of porcine insulin (MW = 5777.7 u) (Fig. 9A) and NC-bound sample (Fig. 9C). Both these spectra were obtained with the deceleration grids (V_E in Fig. 1) set to the flight-tube potential (0 V). Under these conditions no ions which undergo metastable decomposition in the flight tube are rejected [19] so that these spectra give "snapshots" of the ion

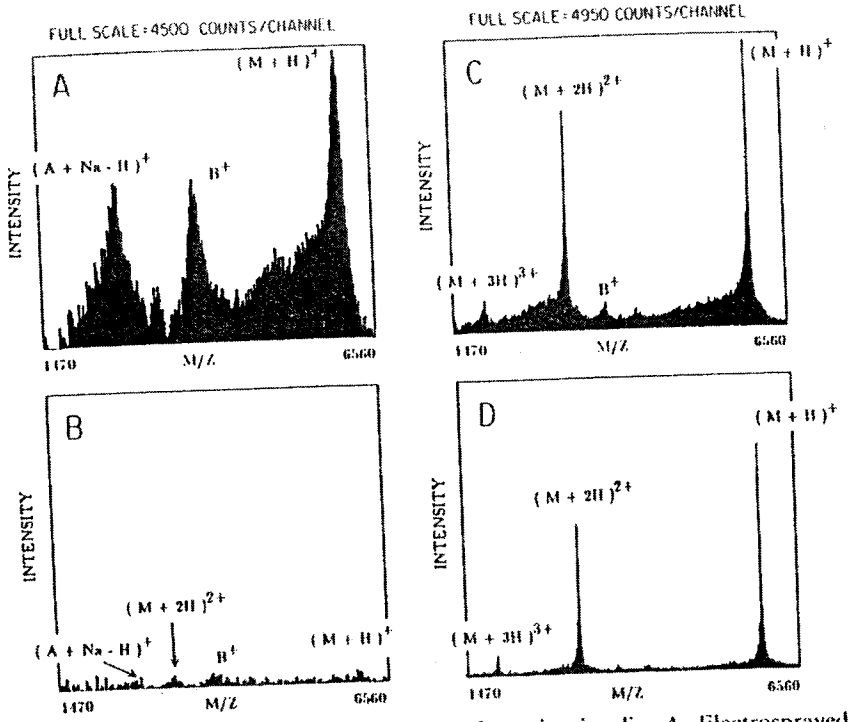

Fig. 9. Partial time-of-flight mass spectra of porcine insulin. A, Electrosprayed sample. No metastable suppression applied, $V_{dec}/V_{acc} = 0.0$ kV/10.0 kV. Run time = 287 min. B, Electrosprayed sample. Metastable suppression applied, $V_{dec}/V_{acc} = 8.4$ kV/10.0 kV. C, Nitrocellulose-bound sample. No metastable suppression applied, $V_{dec}/V_{acc} = 0.0$ kV/10.0 kV. Run time = 61 min. D, Nitrocellulose-bound sample. Metastable suppression applied, $V_{dec}/V_{acc} =$ 9.0 kV/10.0 kV.

populations in the time range between 2×10^{-7} s and 4×10^{-7} s after the ion-forming event. To accentuate the ion peaks, the smooth, featureless continua were subtracted from these spectra. Comparison of Fig. 9A and 9C revealed several striking differences between the spectra obtained using the two different sample preparation techniques. The spectrum obtained with the NC-bound sample exhibits much sharper peaks, a much smaller intensity of fragment ion species, a lower intensity of ions comprising the broad features between the various peaks, and a considerably higher intensity of doubly and triply charged (protonated) intact peptide ions. The data shown in Fig. 9A and 9C are consistent with a considerably lower-energy injection into the protonated porcine insulin ions desorbed from NC compared with the corresponding ions desorbed from bulk electrosprayed layers. Further information on the relative degree of excitation of insulin ions desorbed from the two different sample preparations was obtained by a study of the

metastable fragmentation of the ions during transit through the 3-m flight tube. Such flight tube fragmentation reactions occur for the $(M + H)^+$ ion at times greater than 3.8×10^{-7} s but less than 1.7×10^{-4} s after the ion-forming event. The spectrum shown in Fig. 9B was obtained from the same electrosprayed sample as that shown in Fig. 9A except that a potential was applied to the deceleration grid E (Fig. 1) sufficient to reject the majority of ions which undergo fragmentation in the flight tube. Clearly, very few ions which survive acceleration survive their subsequent transit of the flight tube, e.g. only 2.6% of $(M + H)^+$ ions. This finding is in sharp contrast to the observed survival rate of porcine insulin ions desorbed from NC. Figure 9C shows the partial spectrum from NC-bound insulin with no metastable suppression, and Fig. 9D shows the corresponding spectrum from the same sample with metastable suppression. Again, the ions constituting the broad features between the discrete peaks largely disappear. The $(M + H)^+$ ions, however, have in this case a measured survival rate of fully 78%. These data provided striking evidence that protonated insulin molecules desorbed from NC contain considerably less internal energy than do the corresponding species desorbed from bulk insulin. The detailed reasons for the reduced excitation from NC remain to be elucidated. However, as previously suggested [21,23,24], reduction of the binding energy of the molecules of interest to other molecules and to the surface is probably the dominant factor. Improvements in our undertaking and control of the binding of biomolecules to surfaces holds the prospect of increasing our control over the amount and type of fragmentation incurred during desorption.

We also found that the relative survival probability of polypeptide ions desorbed from NC by fission fragments decreases as a function of increased polypeptide molecular weight. Thus, the injection of an excessive amount of energy during the ion-induced desorption and ionization processes still severely limits the quality of mass spectra obtained from polypeptides with molecular weights > 10000 u, as can be seen, for example, from the partial mass spectrum of horse heart cytochrome C (MW = 12361 u) shown in Fig. 10A.

In addition, we were able to demonstrate, for the first time, that a substantial fraction of the slow unimolecular fragmentation reactions of multiply protonated polypeptides gives rise to two charged fragmentation products rather than a multiply charged fragment and a neutral fragment. This finding confirmed our expectation, based on general energetic and statistical considerations, that the multiple charges would frequently be shared between the fragmentation products. Figure 10B shows the spectrum of fragmentation products which arise exclusively from dissociation of multiply protonated parent molecule ions into two charged fragments. All other ions have been excluded from this mass spectrum by the application of

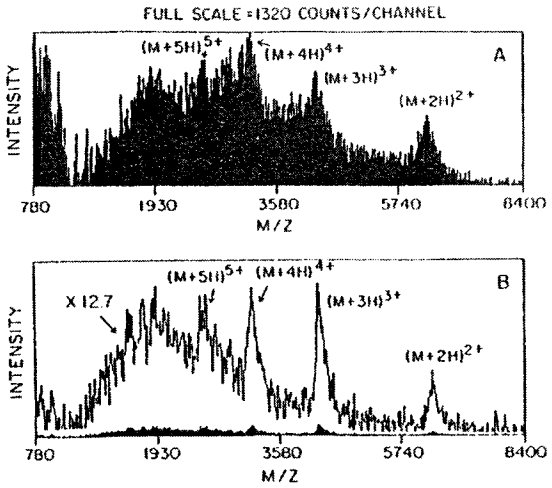

Fig. 10. Time-of-flight mass spectra of horse heart cytochrome C deposited on nitrocellulose showing the region containing the multiply protonated ion peaks. A, No metastable suppression applied, V_{dec}/V_{acc} = 0.0 kV/5.0 kV. B, Metastable suppression applied, V_{dec}/V_{acc} = 5.3 kV/5.0 kV. Filled-in spectrum has been normalized in time with respect to the spectrum shown in A. Unfilled-in spectra is magnified in intensity by a factor of 12.7 compared with the filled-in spectrum.

a potential (V_{dec}) to the deceleration grid with a magnitude greater than that of the acceleration potential (V_{acc}) (see Eq. 1).

COMPARISON OF MASS SPECTRA OBTAINED WITH MeV AND keV ION BOMBARDMENT

Shortly after ^{252}Cf fission fragments with energies of ca. 100 MeV were shown to be highly effective for desorption and ionization of involatile molecules [1,2], Benninghoven and co-workers [25–27], using a magnetic deflection instrument, demonstrated that ions with energies four orders of magnitude lower than fission fragments (i.e. a few keV) were also effective for production of ionized gas-phase molecules from organic solids, at least for compounds with molecular weights < 300 u.

In 1980, together with Standing and Ens at the University of Manitoba, we undertook to compare closely the relative properties and merits of these two techniques [28] by obtaining mass spectra of a series of compounds using the same samples mounted on the same sample foils in two similar time-of-flight mass spectrometers, the Rockefeller University fission fragment instrument (described earlier in this paper) and the pulsed keV ion bombardment mass spectrometer constructed by Chait and Standing at the University of Manitoba [29]. No direct comparison of this type had previ-

ously been carried out. Furthermore, although fission fragment mass spectrometers had been demonstrated to produce significant quasi-molecular ion yields from a wide range of large, involatile, and fragile molecular species, the mass spectral data base for low-energy (keV) ion bombardment was much more limited. Indeed, no spectra of compounds with a mass greater than 350 u had been reported in the literature for keV energy bombardment. We therefore determined the positive and negative mass spectra with both modes of ionization for alanine, arginine, sucrose, guanosine, 5′-adenosine monophosphate, adenylyl-(3′ → 5′)-cytidine (ApC), tetrabutylammonium iodide, and vitamin B_{12} (cyanocobalamin). A very high degree of similarity was observed in the spectra obtained by the two ionization methods for all of these compounds. As an example, Fig. 11A and 11B give, respectively, comparisons of the positive and negative ApC spectra. The consistent similarity of the observed patterns of ions was superficially surprising, as the major energy loss process for fission fragments (electronic stopping, i.e. energy loss by excitation and ejection of sample atomic electrons) is entirely different from that for low-energy (keV) ions (nuclear stopping, i.e. energy loss by elastic scattering from sample atoms) [30]. However, as the precise roles of electronic and nuclear stopping in the desorption and ionization of condensed phase organic molecules have not yet been fully elucidated, the detailed reasons for the close resemblance remain unclear. What we can deduce from the similarity of the observed spectra is that both ionization techniques produce gas-phase ions with similar distributions of internal energy for all the organic compounds studied, and that if initial differences do exist between the two methods, memory of these differences is largely lost on the time-scale relevant to the formation of the major observed ion species.

When we carried out this comparison it was not possible to evaluate properly the relative analytical utility of the two techniques, as we had not determined their relative ion production yields and sensitivities. It seemed clear, however, that the high fluxes available from the low-energy ion gun and the ability to focus the low-energy ions to a small diameter on the sample foil could lead to significant improvements in the working sensitivities. The subsequent development of fast atom bombardment mass spectrometry (FABMS) by Barber and co-workers [31,32] dramatically increased interest in keV energy bombardment. Their discovery that compounds suspended in a nonvolatile liquid matrix give rise to long-lived and relatively intense secondary ion beams under high flux bombardment conditions, allowed for the ready use of conventional deflection and quadrupole mass analyzers, and has made FABMS the most used mass spectrometric method for the analysis of involatile organic compounds. For a number of reasons we have continued to concentrate our efforts on examining solid samples.

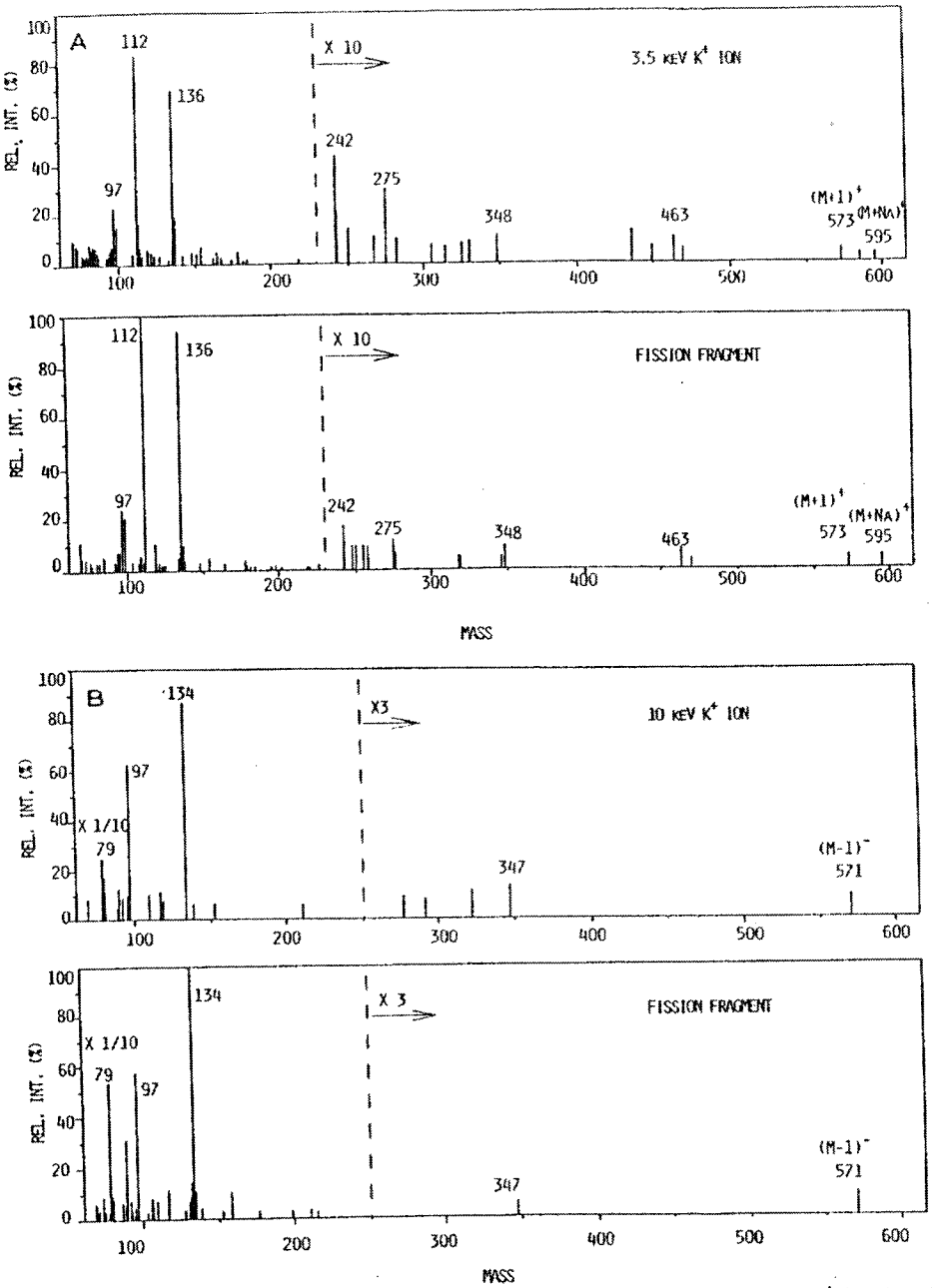

Fig. 11. A, Adenylyl-(3′ → 5′)-cytidine positive ion spectra: upper, 3.5-keV K^+ ion bombardment; lower, ^{252}Cf fission fragment bombardment. B, Adenylyl-(3′ → 5′)-cytidine negative ion spectra: upper, 10-keV K^+ ion bombardment; lower, ^{252}Cf fission fragment bombardment.

These include the fact that such solid samples interface most easily with the simple and efficient time-of-flight mass analyzer, that very small amounts of sample are required for the analysis (a monolayer of material is optimum in many cases), and that background and chemical effects related to the liquid matrix are absent. Recently we have directly compared the relative high- and low-energy bombardment quasi-molecular ion yields for a series of peptides (MW = 500–5700) prepared as solid films by electrospray deposition [33]. As in our previous comparison [28], we observed that the pattern and shapes of the quasi-molecular ion peaks and the shape of the smooth continuum continues to be remarkably similar in the spectra using the two different energy bombarding ion species. A significant difference between the spectra obtained with the two methods is also observed. The ratio of the quasi-molecular ion yield to background decreases faster as a function of increasing mass for keV energy bombardment than for fission fragment bombardment. Fission fragments were observed to have a clear advantage in this respect when compared with keV ion bombardment; this suggests a higher upper mass limit for high-energy particle bombardment. Figure 12 shows the relative quasi-molecular ion yields as a function of mass for incident fission fragments and 8 keV Cs^+ ions. The curves are normalized at leucine enkephalin (MW = 556 u); only the dependence on mass is indicated, not absolute yields. In general, the data indicate a decrease in yield with increasing mass. The decrease is faster for keV bombardment. For the data shown in Fig. 12 we have taken the sharp (stable) component of the spectral peak as the quasi-molecular ion yield because its origin is well understood and it is the most useful portion of this part of the spectrum. However, for the low-energy spectra of the two highest molecular weight compounds (β-endorphin and insulin), no sharp component is distinguishable from the broad (metastable) component so that only upper limits to the yield are given. For both bombarding energies, the data indicate that the yield falls off more slowly for the broad (unstable) component than for the sharp (stable) component. Further, when the broad component is considered, the difference between the yield curves for high- and low-energy bombardment is smaller (Fig. 13).

Most recently we have extended these yield comparisons to samples prepared by adsorption to nitrocellulose [34]. Differences in the relative quasi-molecular ion yields between fission fragment and keV Cs^+ ion bombardment were reduced significantly by the use of the nitrocellulose bound peptide samples rather than electrosprayed samples (Fig. 13). For the first time, intact protonated molecule ions of a compound as large as bovine insulin were detected by keV energy bombardment of solid samples. Thus nitrocellulose extends the useful mass range which can be studied with low-energy ions to proteins with molecular weights between 5000 and 10000

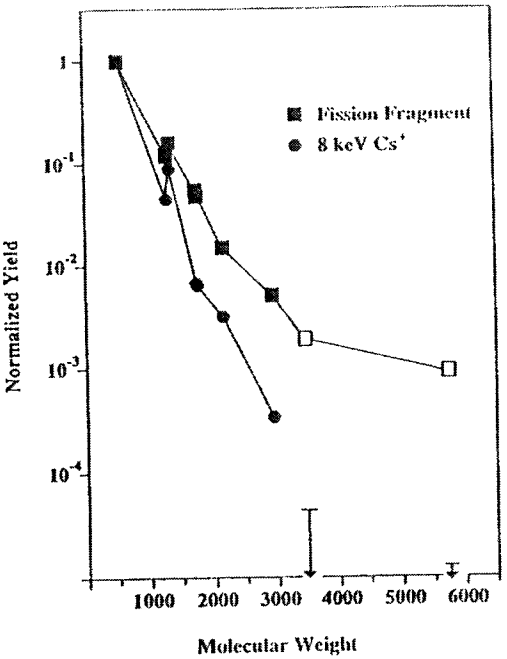

Fig. 12. Dependence of the quasi-molecular ion yield (using the sharp component of the peaks) on molecular weight for a series of peptides bombarded with ^{252}Cf fission fragments (squares) and with 8-keV Cs^+ ions (circles). Data obtained on the two highest molecular weight compounds with kiloelectronvolt incident ions are given as error bars to indicate the upper limits, as sharp peaks were not observed. Post-acceleration was used for the data points depicted with open symbols and error bars; no post-acceleration was used for the filled symbols. With the exception of the upper limits, the statistical error is smaller than the size of the symbol representing the datum. The curves are normalized to the yield for leucine-enkephalin; the data give no information on absolute yields.

u. For still higher molecular weight proteins desorbed from nitrocellulose, Ens et al. [35] have demonstrated that fission fragments continue to have a clear advantage.

We have also compared the effective sensitivities of the two bombardment techniques for a series of peptides (molecular weight range 1000–6000 u) desorbed from nitrocellulose [36]. The comparison in this case was made using 30 keV indium ions in a pulsed ion bombardment time-of-flight mass spectrometer constructed at The Rockefeller University [37] and the previously described fission fragment instrument. The pulsed ion bombardment mass spectrometer was designed to achieve very high sensitivity by using a tightly focused (to a diameter of 0.1 mm), high-intensity primary ion beam to bombard the sample of interest, which can be concentrated onto a small area. The low-energy instrument was found to have a sensitivity advantage

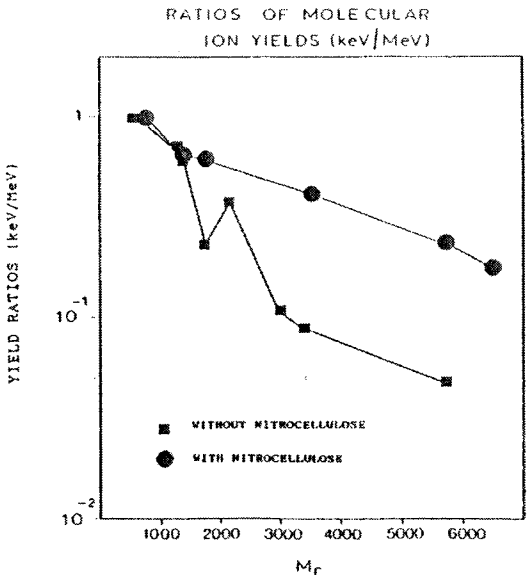

Fig. 13. Ratio of keV/MeV quasimolecular ion yield dependence on molecular weight with a nitrocellulose substrate (circles) compared with an aluminized polyester substrate (squares). Curves are normalized to leucine-enkephalin-arginine and leucine-enkephalin, respectively. The quasimolecular ion yields were taken as the sum of the broad (unstable) component and the narrow (stable) component of the peak.

of a factor of 40 over the fission fragment instrument, which is simply related to the fact the same amount of sample could be deposited on a 40 times smaller area on the sample probe of the former device. Thus, for example, 20 fmol of arginine vasopressin (MW = 1083) introduced into the low-energy instrument gave an $(M + H)^+$ peak with a signal-to-noise ratio of 20 : 1 for a 30 min run. Similar high sensitivities have been observed previously for compounds with molecular weights < 2000 u introduced on acid-etched or sputter-cleaned metal surfaces [37,38]. For all the compounds investigated, the QM ion yield passed through a maximum when the sample introduced into the low-energy mass spectrometer was in the range 2–10 pmol. By contrast, this optimum amount of introduced sample was typically 100–1000 pmol in the case of the fission fragment instrument. In applications where only picomolar amounts of sample are available, the run times can therefore be significantly shorter in the low-energy instrument.

MASS SPECTROMETRY OF MICROSCALE CHEMICAL REACTION PRODUCTS OF ORGANIC SOLIDS AND SURFACE-BOUND ORGANIC MOLECULES

Chemical reactions that take place at the surface of organic solids or on organic molecules bound to surfaces are of interest in a wide range of

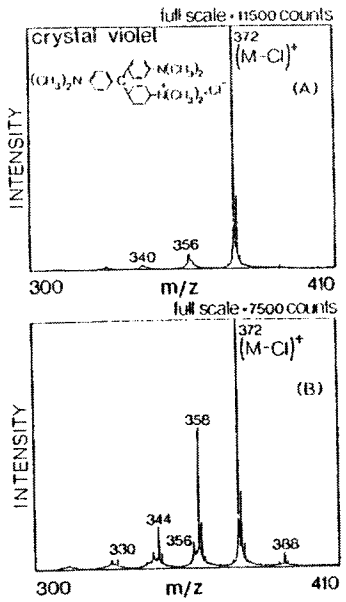

Fig. 14. Partial positive ion spectra of film of crystal violet A unirradiated and B irradiated with visible-wavelength photons.

different areas, including the long-term stability of drugs, the degradation of plastics, the effects of gaseous pollutants on biological systems, catalysis, and a variety of different analytical chemical procedures. In 1985 we discovered a new technique for detecting and investigating such reactions [39]. During the course of a ^{252}Cf ionization mass spectrometric investigation of the triphenylmethane dye crystal violet, we inadvertently exposed a thin solid electrosprayed film of the dye to light in the presence of air after the initial mass spectrometric analysis. Subsequent mass spectrometric re-analysis of the original dye film demonstrated with great clarity that the compound had undergone extensive chemical transformations. The observation suggested the following general procedure:

(1) a thin film of the organic compound of interest is deposited on a metallic substrate;

(2) the film is then analyzed (essentially nondestructively) by ion bombardment mass spectrometry;

(3) the same film is then exposed to the reagent(s) of interest, which causes reaction to occur;

(4) the chemically modified film is then re-analyzed mass spectrometrically.

Figure 14 shows the results of the photochemical transformation of crystal violet described above, but performed under controlled conditions. Figure

14A shows the high-mass portion of the mass spectrum of crystal violet before the photon irradiation of the dye film. The spectrum exhibits an intense intact positive ion peak at m/z 372 and several less intense fragment ion peaks (e.g. at m/z 356 and 340) arising from successive loss of methane. Figure 14B shows the spectrum obtained from the same film after a brief irradiation with visible wavelength photons in an atmosphere of O_2 with H_2O present. The peaks at m/z 358, 344, and 330 arise from three photodemethylation products of crystal violet. The small peak at m/z 388 is probably the $(M-H)^+$ ion of the carbinol base of crystal violet, which also appears to be formed as a photoproduct. Clearly, the amount and the specificity of the information about the chemical reaction under study is high.

To establish the generality of the technique and to investigate some applications of the procedure, the surface reactions of several organic solids were investigated with three major reagent classes:

Photons

Irradiation of rhodamine B under the same conditions as those for crystal violet gave analogous de-ethylation photoproducts with a similar yield [40]. The spectrum of unirradiated diethylstilbestrol exhibits an intense molecular ion peak at m/z 268. Irradiation of the sample with 254-nm photons in air yielded a major product of unknown structure which produces an intense peak at m/z 266. We have also investigated photon-induced reactions on several other organic compounds (see Table 1), and in each clearly detected photoproducts distinct from the starting material.

Light reactive gases

Exposure of a variety of compounds (see Table 1) to O_3, NO, NO_2, Br and HCl demonstrated that the production of new materials could be sensitively followed and their masses readily identified [39–41]. Thus, for example, unsaturated fatty acid salts when exposed to ozone undergo cleavage at the double bond(s) to yield aldehyde and carboxylic acid products. Figure 15 shows the high-mass portion of the mass spectrum of the sodium salt of vaccenic acid $[CH_3(CH_2)_5CH{=}CH(CH_2)_9COONa]$ before and after exposure of the thin film to ozone. Before exposure, the spectrum is dominated by the $(M + Na)^+$ ion at m/z 327, as shown in Fig. 15A. After exposure of the sample to a 1% O_3 in O_2 mixture for 2 s the spectrum shown in Fig. 15B is obtained. The $(M + Na)^+$ peak has disappeared, indicating complete reaction of the starting material, and is replaced by three new peaks which correspond to reaction products of the ozone with the fatty acid salt. The

TABLE 1

Summary of gas–solid chemical reactions investigated with the microscale reaction mass spectrometry probe

Reactions of	With
Photons, O_2, H_2O	Crystal violet, rhodamine B, methylene blue, rose bengal, rose bengal ethyl ester, avermectin $B1_a$, diethyl-stilbestrol, *m*-coumaric acid, biliverdin
Ozone	26-Hydroxycholesterol; desoxycorticosterone hemisuccinate; pregnenolone; dihydrocholesterol; cholesterol; somatostatin; cystine dimethyl ester dihydrochloride; cysteine; nalaxone HCl; leucine-enkephalin; oxidized glutathione; S,S-dimethyl reduced oxytocin; oxytocin; bilirubin; crystal violet; the sodium salts of *cis*-vaccenic acid, *trans*-vaccenic acid, petroselinic acid, oleic acid, elaidic acid, linolelaidic acid, linoleic acid, linolenic acid, nervonic acid; a series of gangliosides
NO_x	19-Hydroxycholesterol, 20-hydroxycholesterol, 26-hydroxycholesterol, vaccenic acid sodium salt, oleic acid sodium salt
Phenylisocyanate	Leucine-enkephalin
Bromine	Vaccenic acid sodium salt, petroselinic acid sodium salt
HCl	Petroselinic acid sodium salt
Edman reaction reagents	Leucine-enkephalin

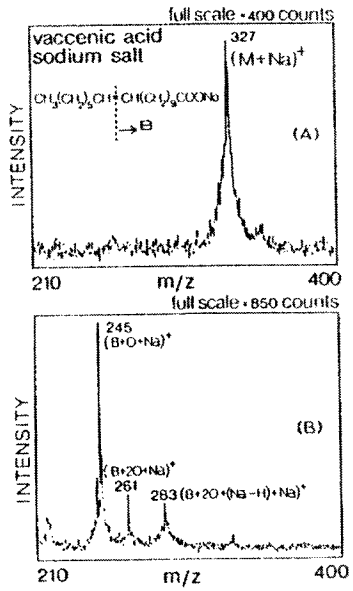

Fig. 15. High-mass portion of the spectrum of vaccenic acid sodium salt taken (A) before and (B) after exposure of the sample film to a 1% O_3 in O_2 mixture for 2 s.

product peaks which occur at m/z 245 ($OHC(CH_2)_9COO\text{-}\dot{N}aNa^+$), m/z 261 ($HOOC(CH_2)_9COO\text{-}\dot{N}aNa^+$), and m/z 283 (the $(M + 2Na - H)^+$ ion corresponding to the m/z 261 ion) unambiguously defined the position of the double bond. The mass spectra after ozone exposure of a series of monounsaturated positional isomers of vaccenic acid as well as of a set of polyunsaturated fatty acid salts (containing as many as four double bonds) similarly yield the position(s) of all the double bonds present. The present surface reaction probe thus appears to constitute a rapid, sensitive and unambiguous technique for determining double bond position(s) in non-volatile compounds.

Complex vapors

To demonstrate the feasibility of carrying out and detecting on a surface film products of a reaction involving complex gaseous reagents, we carried out and monitored mass spectrometrically the coupling and cleavage steps of the Edman sequencing reaction on the terminal residue of the pentapeptide leucine-enkephalin [39].

The general properties of the mass spectrometric surface reaction probe are summarized as follows.

Sensitivity is high; our experience is that 10^{-9}–10^{-15} mol of material can be measured in solid-phase particle bombardment mass spectrometry (the sensitivity depends on the compound under investigation). Low yields (1–2%) of product can be detected reliably (e.g. measured value for the product with m/z 388 in Fig. 14 is 1.5%). The method has a high surface specificity as ion bombardment mass spectrometry is highly surface selective. The mass spectrometric analysis is essentially nondestructive. The analyses are rapid, as many of the mass spectra of the compounds given in Table 1 required a measurement time of < 10 min. In the present system it is not possible to obtain the mass spectra of volatile compounds and volatile reaction products, as they are pumped away.

The microchemical surface reaction probe was originally developed for use with gas-phase reagents. To extend the technique for use with condensed-phase reagents, it is necessary to immobilize the compounds under study so that they are not washed away. We found that the nitrocellulose peptide and protein binding matrix developed by Sundqvist, Roepstorff and co-workers [21] was well suited for this purpose. First, many compounds can be effectively immobilized by relatively tight noncovalent binding to the nitrocellulose surface and at the same time yield a good mass spectrometric response. Second, adsorption to NC is a convenient and an easy method for deposition of submonolayer to monolayer amounts of sample on a surface. The sample or reaction products arising from the sample can then be

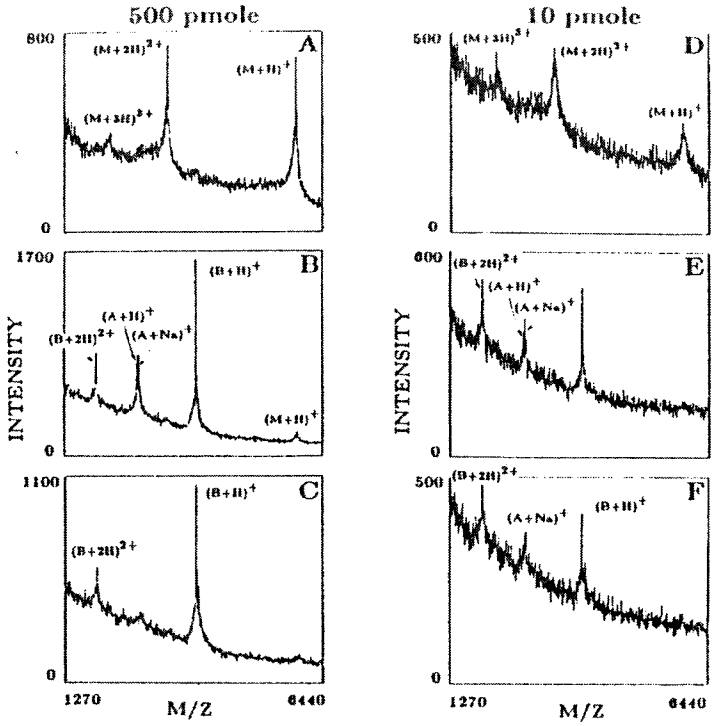

Fig. 16. Reduction of disulfide bonds in surface adsorbed bovine insulin. ^{252}Cf time-of-flight mass spectra of A, 500 pmol sample before reaction; B, after 5.0 min DTT reaction; C, after H_2O rinse of reacted sample; D, 10 pmol sample before reaction; E, after 5.0 min DTT reaction; F, after H_2O rinse of reacted sample. Spectra accumulation times: (A–C) 15 min, (D–F) 30 min.

sensitively monitored by the highly surface sensitive ion bombardment probe.

Our first use of the technique with condensed-phase reagents involved cleavage reactions of the disulfide bonds in bovine insulin, cyclic somatostatin, and conotoxin G1, using the reducing agent 1,4-dithiothreitol [42]. Figure 16A shows the high-mass portion of the fission fragment mass spectrum obtained from 5×10^{-10} mol of bovine insulin deposited on NC, before chemical treatment. The two dominant peaks correspond respectively to the singly and doubly protonated molecule ions of insulin. Figure 16B shows the mass spectrum obtained from the same sample foil after DTT treatment for 5.0 min. The disappearance of the protonated molecular ion peaks and the appearance of a series of lower mass product peaks corresponding to the reduced A and B chains of insulin indicates that the reduction reaction has progressed almost to completion. Figure 16C shows the spectrum from the same sample foil after the surface was thoroughly

washed with water. The peaks corresponding to the A-chain ions have disappeared, indicating that the A-chain products are not strongly bound to the NC and are removed by the washing. Similar experiments performed with smaller amounts of insulin showed that the reduction reaction can be successfully effected as the surface concentration is lowered (Fig. 16D–F). All of these results demonstrate that the reductive cleavage reaction occurs rapidly on surface-bound insulin and that the signal-to-noise ratio is still adequately high at the 10^{-11} mol level to allow ready identification of the reaction products. Similar results were obtained from the reduction of somatostatin (containing one disulfide bond) and conotoxin G1 (containing two disulfide bonds) in which the cyclic molecules were effectively converted into their linear forms with molecular weights respectively 2 and 4 u higher than that of the reactants. In subsequent work, with Kent and coworkers [43], we used this technique to demonstrate that chemically synthesized transforming growth factor alpha (MW = 5546.3) contained three intact disulfide bonds (by mass measurements before and after reduction, which showed a mass gain of 5.9 u).

More recently, we have investigated the utility of the method for measurement of enzyme-catalyzed reactions of surface-bound peptides and proteins [44]. Thus, for example, inspection of the mass spectra of the nonapeptide bradykinin taken before and after incubation with carboxypeptidase Y (CPY) (Fig. 17) provides a clear indication of the masses and relative amounts of the residual peptide products formed from the successive carboxyl-terminal amino acid hydrolyses. Before any reaction, the mass spectrum (Fig. 17A) of an approximate monolayer (10^{-9} mol) of bradykinin adsorbed onto a thin film of nitrocellulose is dominated by a single peak with a measured m/z of 1060.7, which corresponds to the protonated peptide molecule. After reaction of the peptide layer with 10^{-11} mol of CPY for 5 min, the mass spectrum (Fig. 17B) exhibits a series of additional peaks which correspond to the protonated reaction products arising from the loss, respectively, of 1, 2, 4, and 5 C-terminal residues from bradykinin. This example illustrates the potential utility of the present method for C-terminal sequence determinations of peptides. We have performed similar analyses using CPY with angiotensin II, β-endorphin, insulin B-chain, and insulin, and we find that, in all cases, products resulting from the removal of C-terminal residues are observed and can be identified. We also demonstrated that such enzyme-catalyzed reactions could, in certain cases, be successfully carried out and monitored on as little as 1 pmol of surface-bound peptide [44].

Trypsin is an endopeptidase which hydrolyses peptides on the C-terminal side of the basic amino acid residues lysine and arginine. We have investigated the use of the surface reaction probe to identify the resulting tryptic

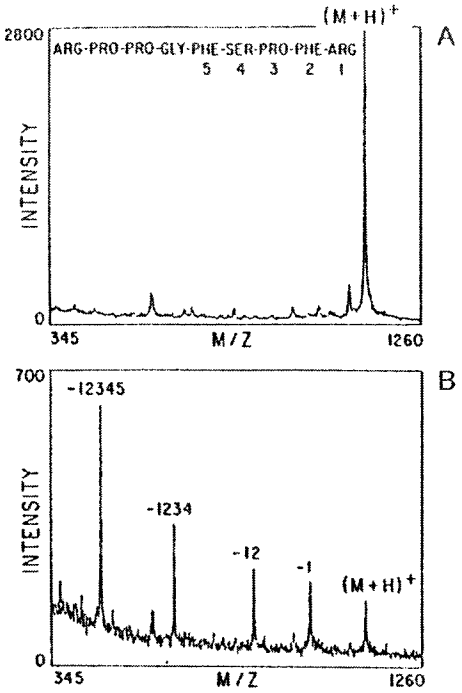

Fig. 17. ^{252}Cf fission fragment ionization time-of-flight mass spectra of bradykinin, bound to a nitrocellulose surface, taken before (A) and after (B) incubation with carboxypeptidase Y. A, Partial mass spectrum of unreacted bradykinin. The solid peptide sample film was prepared by applying 10^{-9} mol of bradykinin to a thin film of nitrocellulose. B, Partial mass spectrum of bradykinin after a 5 min incubation with carboxypeptidase Y at 41°C. The peaks labeled −1, −12, −1234 and −12345 correspond to protonated peptides resulting from the loss of respectively 1, 2, 4 and 5 carboxyl-terminal residues from bradykinin.

fragment from NC surface-bound vasoactive intestinal peptide, dynorphin, bovine insulin B-chain, and porcine proinsulin. In each case, products resulting from the tryptic digestion were readily observed and determined mass spectrometrically. Thus, for example, Fig. 18 shows the mass spectra obtained from 1.7×10^{-10} mol of porcine proinsulin adsorbed on NC before and after reaction with trypsin. Before reaction (Fig. 18A) the high-mass portion of the mass spectrum is dominated by ion peaks corresponding to the addition of 1, 2, 3, and 4 protons to proinsulin. After reaction of the same foil with trypsin these four peaks largely disappear from the spectrum and are replaced by a series of lower molecular weight protonated tryptic fragment product peaks (Fig. 18B). The measured m/z values of these tryptic fragment ions are given in Table 2 together with the masses calculated for the postulated ions given in column 2 of the table. Peaks A, B, D, and F of Fig. 18B correspond to readily rationalized tryptic

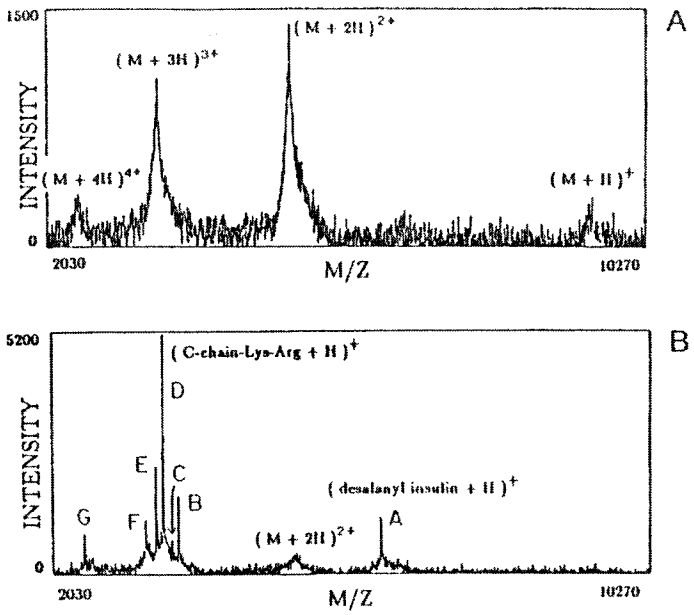

Fig. 18. Mass spectra of porcine proinsulin before and after incubation with trypsin. A, Partial mass spectrum of 1.6×10^{-10} mol porcine proinsulin before any reaction. B, Partial mass spectrum of proinsulin after incubation with trypsin for 12 min at 38°C. The postulated identities of the ions giving rise to the peaks labeled A–G are given in Table 2, together with their measured and calculated m/z values.

fragment ions. We do not know the identity of peak G. Peaks C and E are respectively 71 ± 1 u below peaks B and D and arise from a previously unobserved genetic variant of porcine proinsulin. The presence of a genetic variant in the porcine proinsulin sample was confirmed by direct mass spectrometric detection of the doubly and triply protonated intact variant

TABLE 2

Peak no.	Postulated ion identity	Calculated mass-to-charge ratio	Measured mass-to-charge ratio	Δ
A	(Dealanyl insulin + H)$^+$	5707.7	5707.5	−0.2
B	(Arg-C-peptide-lys-arg + H)$^+$	3185.4	3186.2	+0.8
C	(Arg-C-peptide-lys-arg − 71 + H)$^+$	3114.4	3115.3	+0.9
D	(C-Peptide-lys-arg + H)$^+$	3029.3	3029.1	−0.2
E	(C-Peptide-lys-arg − 71 + H)$^+$	2958.3	2957.6	−0.7
F	(Dealanyl insulin + 2H)$^{2+}$	2854.4	2855.0	+0.6
G	Reaction product not identified		2274.7	

molecule. The site and nature of the variation was deduced from additional mass spectrometric measurements and sequence analysis of chromatographically separated enzymatically generated fragments of porcine proinsulin [45]. This example illustrates the detailed information which can be readily extracted from a small quantity of protein using the above-described method.

In separate experiments, trypsin-catalyzed hydrolysis reactions of dynorphin carried out in the presence of ^{18}O-labeled water allowed the rapid and unambiguous identification of those tryptic fragments containing the C-terminus of the original peptide. The identification was made on the basis of incorporation or nonincorporation of ^{18}O during hydrolysis.

The general properties of the mass spectrometric enzyme-catalyzed surface reaction probe are summarized as follows. Sensitivity is in the range 10^{-9}–10^{-12} mol of polypeptide. Low yields (< 10%) of reaction product can be reliably detected. The mass spectrometric analyses are practically nondestructive of sample, which allows for reactions to be followed as a function of time and also for sequential reactions to be monitored. These properties make this technique an interesting complement to existing techniques. Beyond that, we believe that it will be a valuable general tool for studying biomolecules.

BIOMEDICAL APPLICATIONS

Over the past 9 years we have used the ^{252}Cf plasma desorption mass spectrometer to assist in the solution of a wide variety of biomedical problems. Many of these applications are quite complex and so cannot be discussed in detail here. However, to provide a flavor of the power and the breadth of this analytical tool we list briefly a sampling of some of the studies to which we have contributed.

(1) Structure elucidation of the 20-residue peptide antibiotic alamethicin I [6]. This application is discussed in detail earlier in this paper.

(2) Determination of the carboxyl-terminal structure of the insect antibacterial peptide, cecropin A [46].

(3) Structure elucidation of trypanothione: a novel bis (glutathionyl) spermidine cofactor for glutathione reductase in trypanosomatids [47].

(4) Structure elucidation of lysine adducts with 16α-hydroxyestrone and cortisol [48].

(5) Structure elucidation of the peptide network of pneumococcal peptidoglycan [49].

(6) Determination of altered peptidoglycan structure in a pneumococcal transformant resistant to penicillin [50].

(7) The complete assignment of the seven disulfide linkages in the hormone-binding protein neurophysin [51–53].

(8) Identification and structural elucidation of N-acetylneuraminic acid-containing gangliosides of cat and sheep erythrocytes [54].

(9) Primary structure elucidation of the peptide mating pheromone *Er*-1 of the ciliate *euplotes raikov* [55].

(10) Influence of ions on the cyclization of the amino terminal glutamine residues of the tryptic peptides of streptococcal PepM49 protein: resolution of the cyclized peptides by HPLC and characterization by mass spectrometry [56].

(11) Analysis of synthetic peptides and proteins [57]. We have found through the analysis of over 800 synthetic peptides and proteins submitted to The Rockefeller University Mass Spectrometric Research Resource by 15 different laboratories in the U.S.A. that PDMS provides an enormously useful, rapid, easy, and definitive method for assessing the correctness of structure and homogeneity of both fully protected and unprotected synthetic peptides and proteins.

(12) Fine tuning synthetic peptide chemistry. PDMS was used to evaluate synthetic peptides for deletions and insertions [58]. The use of homopolymers was introduced to provide a large amplification factor for quantification of by-products, and detection limits for insertion and deletion peptides of 0.02% per step were demonstrated. This has led to an improved analysis of reaction conditions for solid-phase synthesis.

(13) Elucidation of the structure of unwanted peptide by-products occurring in tryptophan-containing synthetic peptides [59]. The technique of enzyme-catalyzed microscale chemical reaction of nitrocellulose-bound peptides ([44] and description given earlier in this paper) was used to produce structurally informative hydrolysis products.

ACKNOWLEDGMENTS

I am indebted to all members of The Rockefeller University Mass Spectrometry Laboratory who have worked on the plasma desorption mass spectrometer, and especially Mr. Louis I. Grace and Mrs. Tanuja Chaudhary. This work was supported by a grant from the Division of Research Resources, NIH (RR00862).

REFERENCES

1 D.F. Torgerson, R.P. Skowronski and R.D. Macfarlane, Biochem. Biophys. Res. Commun., 60 (1974) 616.

2 R.D. Macfarlane and D.F. Torgerson, Science, 191 (1976) 920.

3 B.T. Chait, F.H. Field and W.C. Agosta, presented at the 28th Annual Conf. Mass Spectrometry and Allied Topics, May 1980, New York, p. 657; K.G. Standing, W. Ens,

B.T. Chait and F.H. Field, presented at 28th Annual Conf. Mass Spectrometry and Allied Topics, May 1980, New York, p. 661.
4 R.D. Macfarlane and D.F. Torgerson, Int. J. Mass Spectrom. Ion Phys., 21 (1976) 81.
5 B.T. Chait, W.C. Agosta and F.H. Field, Int. J. Mass Spectrom. Ion Phys., 39 (1981) 339.
6 B.T. Chait, B.F. Gisin and F.H. Field, J. Am. Chem. Soc., 104 (1982) 5157.
7 B.T. Chait and F.H. Field, Int. J. Mass Spectrom. Ion Phys., 41 (1981) 17.
8 R.F. Bonner, D.V. Bowen, B.T. Chait, A.B. Lipton, F.H. Field and W.F. Sippach, Anal. Chem., 52 (1980) 1923.
9 R.D. Macfarlane, D.F. Torgerson, Y. Fares and C.A. Hassel, Nucl. Instrum. Meth., 116 (1974) 381.
10 A. Hedin, P. Hakansson and B.U.R. Sundqvist, Int. J. Mass Spectrom. Ion Processes, 70 (1986) 203.
11 B.T. Chait and F.H. Field, J. Am. Chem. Soc., 106 (1984) 1931.
12 Isotope Products Laboratories, Burbank, CA.
13 Digital Equipment Corp., Merrimack, N.H.
14 L.I. Grace, B.T. Chait and F.H. Field, Biomed. Environ. Mass Spectrom., 14 (1987) 295.
15 C.J. McNeal, R.D. Macfarlane and E.L. Thurston, Anal. Chem., 51 (1979) 2036.
16 M. Mudgett, D.V. Bowen, F.H. Field and T.J. Kindt, Biomed. Mass Spectrom., 4 (1977) 159.
17 P. Roepstorff and J. Fohlman, Biomed. Mass Spectrom., 11 (1984) 601.
18 B.T. Chait and F.H. Field, J. Am. Chem. Soc., 104 (1982) 5519.
19 B.T. Chait, Int. J. Mass Spectrom. Ion Processes, 53 (1983) 227.
20 B.T. Chait and F.H. Field, Int. J. Mass Spectrom. Ion Phys., 65 (1985) 169.
21 G.P. Jonsson, A.B. Hedin, P.L. Hakansson, B.U.R. Sundqvist, B.G.S. Save, P.F. Nielsen, P. Roepstorff, K.-E. Johansson, J. Kamensky and M.S.L. Lindberg, Anal. Chem., 58 (1986) 1084.
22 B.T. Chait, Int. J. Mass Spectrom. Ion Processes, 78 (1987) 237.
23 E.A. Jordan, C.R. Martin, C.J. MacNeal and R.D. Macfarlane, presented at the 32nd Annual Conference on Mass Spectrometry and Allied Topics, San Antonio, 1984, p. 26.
24 E.A. Jordan, R.D. Macfarlane, C.R. Martin, C.J. McNeal, Int. J. Mass Spectrom Ion Processes, 53 (1983) 345.
25 A. Benninghoven, D. Jaspers and W. Sichtermann, Appl. Phys., 11 (1976) 35.
26 A. Benninghoven and W. Sichtermann, Org. Mass Spectrom., 12 (1977) 595.
27 A. Benninghoven and W. Sichtermann, Anal. Chem., 50 (1978) 1180.
28 W. Ens, K.G. Standing, B.T. Chait and F.H. Field, Anal. Chem., 53 (1981) 1241.
29 B.T. Chait and K.G. Standing, Int. J. Mass Spectrom. Ion Phys., 40 (1981) 185.
30 See, e.g., P. Sigmund, in R. Behrisch (Ed.) Topics in Applied Physics, Vol. 47, Springer-Verlag, Berlin, 1981, p. 9.
31 M. Barber, R.S. Bordoli, R.D. Sedgwick and A.N. Tyler, J. Chem. Soc. Chem. Commun. (1981) 325.
32 M. Barber, R.S. Bordoli, G.J. Elliott, R.D. Sedgwick and A.N. Tyler, Anal. Chem., 54 (1982) 645A.
33 W. Ens, D.E. Main, K.G. Standing and B.T. Chait, Anal. Chem., 60 (1988) 1494.
34 F. Lafortune, R. Beavis, X. Tang, K.G. Standing and B.T. Chait, Rapid Commun. Mass Spectrom., 1 (1987) 114.
35 W. Ens, P. Hakansson, B.U.R. Sundqvist, in A. Benninghoven, A.M. Huber and H.W. Werner (Eds.), Proc. 6th Int. Conf. Secondary Ion Mass Spectrometry, SIMS VI, Wiley, Chichester, 1988, p. 623.
36 V. Katta, L.I. Grace, T. Chaudhary and B.T. Chait, presented at 36th ASMS Conf. Mass Spectrom. Allied Topics, San Francisco, June 1988.

37 B.T. Chait and F.H. Field, presented at 32th ASMS Conf. Mass Spectrom. Allied Topics, San Antonio, May 1984.
38 A. Benninghoven, E. Niehuis, T. Friese, D. Greifendorf and P. Steffens, Org. Mass Spectrom., 19 (1984) 7.
39 B.T. Chait and F.H. Field, J. Am. Chem. Soc. 107 (1985) 6743.
40 B.T. Chait and F.H. Field, in J.F.J. Todd (Ed.) Advances in Mass Spectrometry 1985, Part B, Wiley, New York, 1986, p. 1587.
41 B.T. Chait, in A. Benninghoven (Ed.) Ion Formation from Organic Solids (IFOS III), Springer-Verlag, Berlin, 1986, p. 34.
42 B.T. Chait and F.H. Field, Biochem. Biophys. Res. Commun., 134 (1986) 420.
43 D.D.-L. Woo, I. Clarke-Lewis, B.T. Chait and S.B.H. Kent, Protein Engng, submitted.
44 B. Chait, T. Chaudhary and F.H. Field, in K.A. Walsh (Ed.) Methods in Protein Sequence Analysis 1986, Humana Press, Clifton, NJ, 1987, p. 483.
45 B.T. Chait and R.E. Chance, in preparation.
46 D. Andreu, R.B. Merrifield, H. Steiner and H.G. Boman, Proc. Natl. Acad. Sci. U.S.A., 80 (1983) 6475.
47 A.H. Fairlamb, P. Blackburn, P. Ulrich, B.T. Chait and A. Cerami, Science, 227 (1985) 1485.
48 B. Bucala, P.C. Ulrich, B.T. Chait, F.A. Bencsath and A. Cerami, J. Steroid Biochem., 25 (1986) 127.
49 J. Garcia-Bustos, B.T. Chait and A. Tomasz, J. Biol. Chem., 262 (1987) 15400.
50 J. Garcia-Bustos, B.T. Chait and A. Tomasz, J. Bacteriol., 170 (1988) 2143.
51 S. Burman, E. Breslow, B.T. Chait and T. Chaudhary, Biochem. Biophys. Res. Commun., 148 (1987) 827.
52 S. Burman, E. Breslow, B.T. Chait and T. Chaudhary, J. Chromatogr., 443 (1988) 285.
53 S. Burman, D. Wellner, B. Chait, T. Chaudhary and E. Breslow, Proc. Natl. Acad. Sci. U.S.A., 86 (1989) 429.
54 K. Furukawa, B.T. Chait and K.O. Lloyd, J. Biol. Chem., 263 (1988) 14939.
55 S. Raffioni, P. Luporini, B.T. Chait, S.S. Disper and R.A. Bradshaw, J. Biol. Chem., 263 (1988) 18152.
56 K.M. Khadke, T. Fairwell, B.T. Chait and B.N. Manjula, Int. J. Peptide Protein Res., 29 (1989) in press.
57 B.T. Chait, in C.J. McNeal (Ed.), The Analysis of Peptides and Proteins by Mass Spectrometry, Wiley, New York, 1988, p. 21.
58 R.B. Merrifield, J. Singer and B.T. Chait, Anal. Biochem., 174 (1988) 399.
59 S.K. Chowdhury and B.T. Chait, Anal. Biochem., 180 (1989) in press.